MARINE RESERVOIR CORRECTIONS FOR THE INDIAN OCEAN AND SOUTHEAST ASIA

John Southon[1] • Michaele Kashgarian[2] • Michel Fontugne[3] • Bernard Metivier[4] • Wyss W-S Yim[5]

ABSTRACT. We have measured radiocarbon in prebomb known-age shells and coral from the Indian Ocean and southeast Asia to determine marine reservoir age corrections. Western Indian Ocean results show a strong ^{14}C depletion due to upwelling in the Arabian Sea, and indicate that this signal is advected over a wide area to the east and south. In contrast, the surface waters of the South China Sea contain relatively high levels of ^{14}C, due in part to the input of well-equilibrated water masses from the western Pacific. The easternmost regions of the Indian Ocean are also strongly influenced by the flowthrough of Pacific waters north of Australia.

INTRODUCTION

Dissolved inorganic carbon (DIC) in the surface ocean (the mixed layer) is influenced by exchange with both the atmosphere and the radiocarbon-depleted deep ocean (Stuiver and Ostlund 1983) and has a ^{14}C content intermediate between the two. A knowledge of the resulting surface ocean ^{14}C age offset relative to that of atmospheric CO_2—the reservoir age—is essential for dating marine materials. Stuiver and co-workers (Stuiver et al. 1986; Stuiver and Brazuinas 1993; Stuiver et al. 1998) have used a carbon reservoir model to generate a global marine ^{14}C age calibration R(t) that incorporates temporal variations forced by known changes in atmospheric ^{14}C. This calibration is extended through additional regional corrections (ΔR values) for spatial variations in upwelling, water mass mixing, and air-sea gas exchange. Typically, these corrections are determined by dating prebomb known-age marine carbonate.

Prebomb ^{14}C data for the Indian Ocean and adjacent marginal seas are relatively sparse. Broecker (1963) measured ^{14}C depletions of −70‰ and −59‰ in shells collected near Mombasa and north of Bombay (no collection dates or ^{14}C uncertainties given). Other early measurements include data on shells (Gillespie 1977; Rhodes 1980; Delibrias 1980; Bowman 1985) and coral bands (Broecker et al. 1987; Cember 1989; Toggweiler et al. 1991). In recent work, von Rad et al. (1999) measured ^{14}C in known-age forams from varved sediment cores recovered off Pakistan, and Dutta et al. (2001) dated mollusks to determine reservoir ages for seven sites in the Arabian Sea and Bay of Bengal. We know of no published reservoir age data for southeast Asia, though Konishsi et al. (1982) measured ^{14}C time series in two coral heads from Okinawa to the northeast. In this study, we present ^{14}C data from known-age mollusk, gastropod, and coral samples from sites between the Cape of Good Hope and the western Pacific, primarily from the western Indian Ocean and the South China Sea. We discuss these results within the framework of the regional oceanography of the Indian Ocean and southeast Asia.

RADIOCARBON AGE DETERMINATIONS

Prebomb mollusk and gastropod samples for this study are from the collections of the Museum National d'Histoire Naturelle, Paris (MNHN) and the US National Museum of Natural History, Smithsonian Institution, Washington, DC (USNM). Post-bomb samples were obtained from the

[1]Earth System Science Department, 220 Rowland Hall, University of California, Irvine, California, 92697-3100, USA.
 Email: jsouthon@uci.edu.
[2]Center for AMS, L-397, Lawrence Livermore National Laboratory, Livermore, California 94551-9900 USA
[3]Laboratoire des Sciences, du Climat et de l'Environnement, Domaine du CNRS, F-91198 Gif-sur-Yvette Cedex, France
[4]Laboratoire de Biologie des Invertebres Marins et Malacologie, Musuem National d'Histoire Naturelle, 55 Rue de Buffon,
 75005 Paris, France
[5]Department of Earth Sciences, The University of Hong Kong, Pokfulam Road, Hong Kong SAR, China

Hong Kong Museum of History (H), and an approximately 100-year-old *Porites* coral head from the Xisha Islands in the South China Sea was provided by Dr Min Sun of the University of Hong Kong. Samples include MNHN specimens from as early as 1820 (no known-age specimens collected earlier were available, as all records of the French Royal collection were lost during the French Revolution). Documentation included species identification, sampling date or date of entry into the collection, and location, though only regional geographical information (e.g., "Ceylon", "Red Sea") was available in some cases. Some early USNM samples are known to have been collected prior to the dates indicated, but probably by only a few decades at most. For the purposes of this study, we have assumed that the sampling and collection entry dates are equivalent.

The shells were cleaned by washing and grinding the surface. Aliquots a few mm square—large enough to cover at least one entire year of growth—were taken from near the outer (growing) edge of each shell. The carbonate was crushed to a 0.5–1 mm powder, etched with 0.1N HCl to remove 30% of each sample, and subsamples of 10–15 mg were hydrolyzed to CO_2 with 85% phosphoric acid. Calcite blanks were also measured, and duplicate aliquots of several samples were prepared and measured. The CO_2 samples were converted to graphite by hydrogen reduction with an iron or cobalt catalyst (Vogel et al. 1987; Loyd et al. 1991), and ^{14}C was measured at the Center for AMS, LLNL (Southon et al. 1990). Bands from coral slabs were sampled with a Dremel® milling tool and the carbonate powder was treated as above. Separate aliquots were taken for $\delta^{13}C$ measurements, or values of 0‰ (mollusks/gastropods) or −2‰ (*Porites* coral) were assumed based on measured values for other samples.

RESULTS AND DISCUSSION

Indian Ocean ^{14}C and stable isotope results are presented in Table 1. The difference between the conventional ^{14}C age for each sample (Stuiver and Polach 1977) and the model age for the calender year of collection (Stuiver and Braziunas 1993) gives the ΔR corrections, and the uncertainties are assumed to be those of the age determinations. (Note that small offsets appear between the 1986, 1993 and 1998 marine ^{14}C calibrations due to minor changes in model parameters and slight differences in the atmospheric datasets used as model input, but these are negligible compared to ^{14}C measurement uncertainties and natural ΔR variability.) The results are also given as $\Delta^{14}C$, corrected for radioactive decay between the year of collection and AD 1950. An additional correction has also been applied to the $\Delta^{14}C$ data for the 20th century Suess effect—the ^{14}C dilution due to fossil fuel CO_2 uptake by the oceans (Druffel and Suess 1983; Stuiver and Braziunas 1993; see Table 1 footnote)— but note that this is simply an estimate and the actual effect may be more complex and variable (Druffel and Griffin 1993; Druffel 1997).

Indian Ocean

ΔR values are high in almost all of the western Indian Ocean samples, but a 1959 sample from Mauritius shows a negative ΔR, an artifact of bomb ^{14}C uptake in the late 1950s. A sample from Pondicherry in the western Bay of Bengal gave an extremely high ΔR of 495 years, in strong disagreement with our result from the Nicobar Islands and the Bay of Bengal data of Dutta et al. (2001). The rather low $\delta^{13}C$ value of −1.9‰ for the Pondicherry sample, suggestive of fresh water influence, may indicate that this anomalous result is due to geological carbonate input.

Omitting the two outliers and eastern Indian Ocean data from Java, Australia, and the Bay of Bengal discussed below, the results cluster closely around a mean ΔR of 158 ± 68 years (N = 31) (Figure 1), or $\Delta^{14}C$ (Suess-corrected) = −67.3 ± 8.1‰. The ±68-year 1-σ scatter in the data set is only slightly larger than the uncertainties in the individual results, typically ±55 years. This suggests that a rough

Table 1 Prebomb radiocarbon data from this study—Indian Ocean

Sample nrs (CAMS#)[a]	Museum nr	Species (b=bivalve, c=coral, g=gastropod)	Coll. date	Location	Lat (°N)	Long (°E)	δ13C (‰)	Δ14C (‰)	±	Δ14C (Suess corr.)[b]	14C age ± BP	Model age (BP)	ΔR
Western Arabian Sea													
3953	MNHN-C28	*Marcia flammea (b)*	1843	Muscat	23.5	58.6	1.8	−81.4	5.8	−81.4	786 ± 51	501	285
3920	MNHN-C1	*Marcia flammea (b)*	1850	Aden	12.5	45	1.5	−66.9	6.6	−66.9	653 ± 57	496	157
3926	MNHN-C7	*Gafrarium callipygum (b)*	1850	Socotra	12.5	54	0.6	−72.5	6.6	−72.5	702 ± 57	496	206
3929	MNHN-C10	*Pinctada margaritifera (b)*	1897	Muscat	23.5	58.6	1.7	−72.7	6.9	−72.7	658 ± 60	469	189
3938	MNHN-C17	*Irus rugosus (b)*	1920	Perim	12.5	53.3	1.4	−64.7	6.6	−62.7	566 ± 57	465	101
3948+3960	MNHN-C23	*Marcia flammea (b)*	1921	Aden	12.5	45	1.2	−86.3	5.8	−84.3	753 ± 51	466	287
3921	MNHN-C2	*Pinctada radiata (b)*	1921	Aden	12.5	45	1.7	−76.5	7.8	−74.5	668 ± 68	466	202
3924	MNHN-C5	*Tapes deshayesi (b)*	1921	Djibouti	11.3	43	2.4	−64.0	6.6	−62.0	559 ± 57	466	93
Red Sea/Persian Gulf													
3939+3944	MNHN-C18	*Pinctada radiata (b)*	1839	Red Sea[c]	ca. 20	ca. 38	1.7	−59.5	4.5	−59.5	600 ± 38	504	96
3958	MNHN-C33	*Pinctada radiata (b)*	1952	Dohar, Qatar	25.3	51.4	1.8	−77.9	6.0	−67.9	649 ± 53	486	163
Eastern Arabian Sea/Sri Lanka													
3928	MNHN-C9	*Marcia recens (b)*	1836	Bombay	18.8	72.7	0.2	−65.7	6.6	−65.7	656 ± 57	505	151
8693	USNM-90558	*Gastropod*	1887[d]	Bombay	18.9	72.8	0	−62.4	5.5	−62.4	580 ± 50	473	107
3950	MNHN-C25	*Marcia opima (b)*	1841	Goa, India	16.5	73.8	−1.1	−76.2	5.8	−76.2	742 ± 51	502	240
3927+3933	MNHN-C8	*Paphia textile (b)*	1847	Malabar, India	11.3	76	0.6	−63.2	7.5	−63.2	625 ± 64	499	126
3940+3945	MNHN-C19	*Pinctada margaritifera (b)*	1841	Sri Lanka[c]	ca. 7	ca. 80	2.2	−58.6	5.5	−58.6	591 ± 47	502	89
3947	MNHN-C22	*Pinctada radiata (b)*	1874	Sri Lanka[c]	ca. 7	ca. 80	1.1	−70.8	6.2	−70.8	663 ± 53	484	179
3959	MNHN-C34	*Timoclea cochinensis (b)*	1924	Sri Lanka[c]	ca. 7	ca. 80	0.3	−74.7	6.0	−74.7	649 ± 53	465	184
8692	USNM-89612	*Gastropod*	1887[b]	Sri Lanka[c]	ca. 7	ca. 80	0	−56.1	5.5	−56.1	530 ± 50	473	57
3957+3962	MNHN-C32	*Gafrarium scriptum (b)*	1841	Raffles Bay, N.Australia	−11.3	132.4	0.4	−53.6	4.7	−53.6	549 ± 40	502	47

[a]CAMS = Center for AMS, LLNL; MNHN = Museum National d'Histoire Naturelle; USNM = National Museum of Natural History, Smithsonian Institution.
[b]Estimated marine fossil fuel (Suess) effect, per mil: 1959: −16 ± 4; 1952: −10 ± 2; 1945: −8 ± 2; 1925: −2 ± 2; 1920: −2 ± 2; pre-1920: ca. zero.
[c]Location approximate
[d]Collected earlier, assumed this date for calculations

Table 1 Prebomb radiocarbon data from this study—Indian Ocean (*Continued*)[a]

Sample nrs (CAMS#)	Museum#	Species (b=bivalve, c=coral, g=gastropod)	Coll. date	Location	Lat (°N)	Long (°E)	δ13C (‰)	Δ14C (‰)	±	Δ14C (Suess corr.)[b]	14C age ± BP	Model age (BP)	ΔR
Southwest tropical Indian Ocean													
3930+3942	MNHN-C11	*Tapes deshayesi (b)*	1836	Ile de France, Mauritius	−21	56	1.2	−60.9	4.7	−60.9	616 ± 40	505	111
3922+3932	MNHN-C3	*Laevicardium flavum (b)*	1945	Mauritius	−21	56	0.6	−69.3	4.9	−61.3	582 ± 42	480	102
3946	MNHN-C21	*Pinctada margaritifera (b)*	1959[e]	Mauritius	−21	56	1.7	−51.8	6.7	−35.8	418 ± 57	500	-82
3941	MNHN-C20	*Pinctada radiata (b)*	1841	Diego-Suarez, Madagascar	−12.4	49.4	1.0	−67.4	7.0	−67.4	667 ± 60	502	165
3935	MNHN-C14	*Pinctada radiata (b)*	1840	Seychelles	−9.4	47	1.7	−82.7	6.8	−82.7	800 ± 59	503	297
3936	MNHN-C15	*Gafrarium pectinatum (b)*	1840	Seychelles	−9.4	47	2.5	−63.9	6.6	−63.9	637 ± 57	503	134
3949	MNHN-C24	*Pinctada maculata (b)*	1840	Seychelles	−9.4	47	0.0	−56.9	6.7	−56.9	577 ± 57	503	74
3931	MNHN-C12	*Fragum fragum (b)*	1850	Seychelles	−9.4	47	3.6	−53.0	6.7	−53.0	535 ± 57	496	39
3954	MNHN-C29	*Gafrarium pectinatum (b)*	1878	Mahe, Seychelles	−9.4	47	0.8	−66.7	7.2	−66.7	624 ± 62	479	145
3937	MNHN-C16	*Tapes deshayesi (b)*	1874	Mayotte, Comoros	−13.1	45.7	2.1	−62.8	6.6	−62.8	595 ± 57	484	111
3955	MNHN-C30	*Laevicardium biradiatum (b)*	1921	Comoros	−11.6	43.5	0.9	−81.6	5.8	−79.6	712 ± 51	466	246
3934+3943	MNHN-C13	*Pinctada radiata (b)*	1864	Zanzibar	−6.3	39.3	−0.1	−65.7	4.6	−65.7	630 ± 40	490	140
South Africa (E. coast)													
3925	MNHN-C6	*Venerupis corrugatus (b)*	1820	Cape of Good Hope	−34.5	18.6	0.6	−72.8	5.9	−72.8	734 ± 51	522	212
3951	MNHN-C26	*Marcia paupercula (b)*	1945	Natal	−30	31.1	1.4	−80.2	6.5	−72.2	677 ± 57	480	197
Bay of Bengal													
3923	MNHN-C4	*Marcia opima (b)*	1920[d]	Pondicherry, India	12.1	80	−1.9	−109.4	6.3	−107.4	960 ± 57	465	495
6574	USNM-253450	*Thais sp. (g)*	1913[d]	Nicobar Islands	9	94	0	−53.6	7.7	−53.6	480 ± 70	463	17
Other													
6569	USNM-260602	*Thais sp. (g)*	1910	Pelabuhanratu, S. Java	−7.0	106.5	0	−54.9	7.7	−54.9	490 ± 70	462	28
3957+3962	MNHN-C32	*Gafrarium scriptum (b)*	1841	Raffles Bay, N.Australia	−11.3	132.4	0.4	−53.6	4.7	−53.6	549 ± 40	502	47

[a]See previous page for footnotes a through d.
[e]Post-bomb

upper limit for any regional ΔR variations within the western Indian Ocean is $\sqrt{(68^2 - 55^2)}$, i.e., around ±40 years or ±5‰. Since this value also provides an upper limit for any temporal changes, the results suggest that changes in western Indian Ocean reservoir ages over the period 1820–1950 are quite well described by the atmospheric forcing model: there are no indications of major changes in large-scale upwelling over this period.
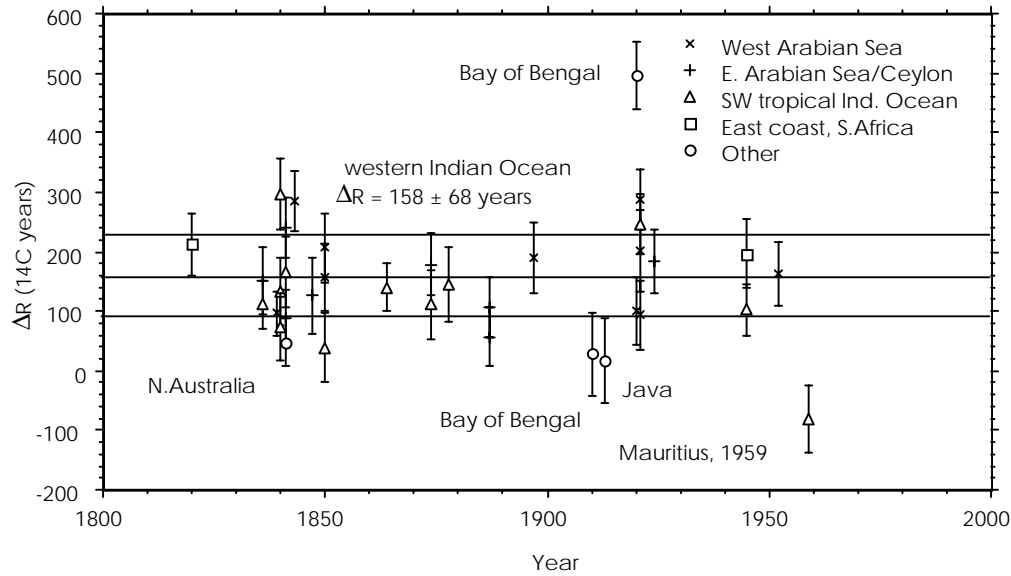

Figure 1 ΔR values from this study for the Indian Ocean and adjacent marginal seas, plotted against the year of collection. Apart from the five identified outliers (see text), the results show little variation above the scatter expected from the uncertainties in the radiocarbon measurements.

Table 2 Δ^{14}C (Suess-corrected) and ΔR—regional means (this study)

Location	Δ^{14}C (‰)	±	ΔR (yr)	±
Indian Ocean				
Western Arabian Sea (N=8)	−73.1	2.8	190	25
Eastern Arabian Sea and Ceylon (N=8)	−66.0	2.6	140	20
Tropical SW Indian Ocean (N=11)	−65.7	2.8	140	25
East coast of South Africa (N=2)	−72.5	4.5	205	30
South China Sea				
South/central S. China Sea (N=10)	−47.4	2.3	−25	20

Regional mean ΔR and Suess-corrected Δ^{14}C values for the western Indian Ocean are shown in Table 2. We have assumed that the values within each region are essentially constant, so that the relevant uncertainty is the standard error of the mean (i.e., $\sigma/\sqrt{N}$). However, some results from within single regions do show substantial scatter; e.g., shells collected in the Seychelles in 1840 and 1850 show a 260-year spread (>4 σ) in reservoir age, and also show large δ^{13}C variations—see Table 1. Whether this indicates real spatial variation within the local mixed layer, fast temporal changes, use of samples from lagoons or estuaries that do not reflect open ocean conditions, or some other cause,

is unclear. It is important to remember when evaluating shell dates that such variations do exist (see also Bhushan et al. 1994; Ingram and Southon 1996; Dye 1995) and that the causes are not always obvious, so that use of regional ΔR values may gloss over substantial variability.

Data from previous studies are summarized in Table 3 and synthesized with our own results in Figure 2. The overall agreement between the different datasets is generally good, though a few clear exceptions exist. A lack of concordance between our results and data from Delibrias (1980) for Mauritius and Madagascar remains unresolved, but we note that Toggweiler et al. (1991) measured extremely variable post-bomb ^{14}C values in Mauritius corals, suggesting that perhaps prebomb ^{14}C levels in these waters also fluctuated. Data from Sri Lanka which also appear discordant are discussed below.

Table 3 Prebomb radiocarbon results from previous studies discussed in the text

Reference	Location	Lat (°N)	Long (°E)	Δ^{14}C (‰) (Suess-corr.)	±	ΔR (yr)	±
Gillespie (1977)[a]	Garden Is., W Australia	−32.3	115.7	−51.8	10	5	80
	Torres Str., Queensland (N=3)	−10	143	−53.1	5.4	31	43
Rhodes et al. (1980)	Gulf of Carpentaria (N=2)	−12	142	−54.2	3.9	41	70
Delibrias (1980)[b]	Mauritius	−20.3	57.5	−47.2	4	-40	35
	Nossibe, NW Madagascar	−13.4	48.5	−41.5	4	-49	35
Konishi et al. (1982)	Okinawa (N=18)	26.4	127.8	−32.8	0.9	-149	7
Bowman (1985)	NW Australia[c] (N=7)	17	123	−58.9	4.4	44	46
Broecker et al. (1987)[d]	Al-Jurayd Is, Persian Gulf	27.2	49.9	−68	8.2	179	66
Cember (1989)	Hurghada, Red Sea (N=2)	27	34	−65.9	5.3	135	42
	Port Sudan, Red Sea (N=2)	20	37	−65.5	5.7	132	45
Toggweiler et al. (1991)[d]	Cocos-Keeling Is.	−12	97	−71	8.4	182	65
	Djibouti[e]	11.3	43	−67.8	8.5	147	68
von Rad et al. (1999)	Off Pakistan (N=2)	24.83	65.92	−77	2.2	218	20
Dutta et al. (2001)	Gujarat (N=2)	22.15	69	−67	5	162	30
	Chilika L., Orissa	19.8	85.5	−39	7	-78	53
	Stewart Sd., Andaman Islands	13	93	−51	4.7	-2	35
	Palk Bay, Tamilnadu (N=3)	9.2	79	−52	2.7	20	20

[a]Original data are δ^{14}C: Δ^{14}C = δ^{14}C−(2×δ^{13}C+50)×(1+δ^{14}C/1000).
[b]Original data are "Apparent ages": radiocarbon ages calculated with 5730-yr half-life, with collection date 1950 subtracted.
[c]Collection dates between 1902 and 1950, assume 1926.
[d]Original data are D^{14}C, though quoted as Δ^{14}C: see Cember (1989)
[e]Collection date pre-WWII, assume 1900.

The combined old and new data indicate that ^{14}C levels in western Indian Ocean surface waters are significantly low compared to the global surface water of the reservoir age model. In broad terms, this is consistent with known oceanographic data. GEOSECS results show that deep Indian Ocean water is strongly depleted in ^{14}C (Stuiver and Ostlund 1983), and vigorous upwelling of deep and bottom water is a feature of the large-scale northern Indian Ocean circulation (Toole and Warren 1993; Ganachaud and Wunsch 2000). In a more detailed view, the intense monsoon-driven upwelling which takes place off the Somali and southern Arabian coasts and to a lesser extent off Pakistan and India (Swallow 1984; Wyrtki 1973) is the basis for the large ΔR values in the Arabian Sea. Several mechanisms combine to propagate the influence of this deep Indian Ocean water contribution not only throughout the Arabian Sea, but also into large areas of the western Indian Ocean and adjacent regions.
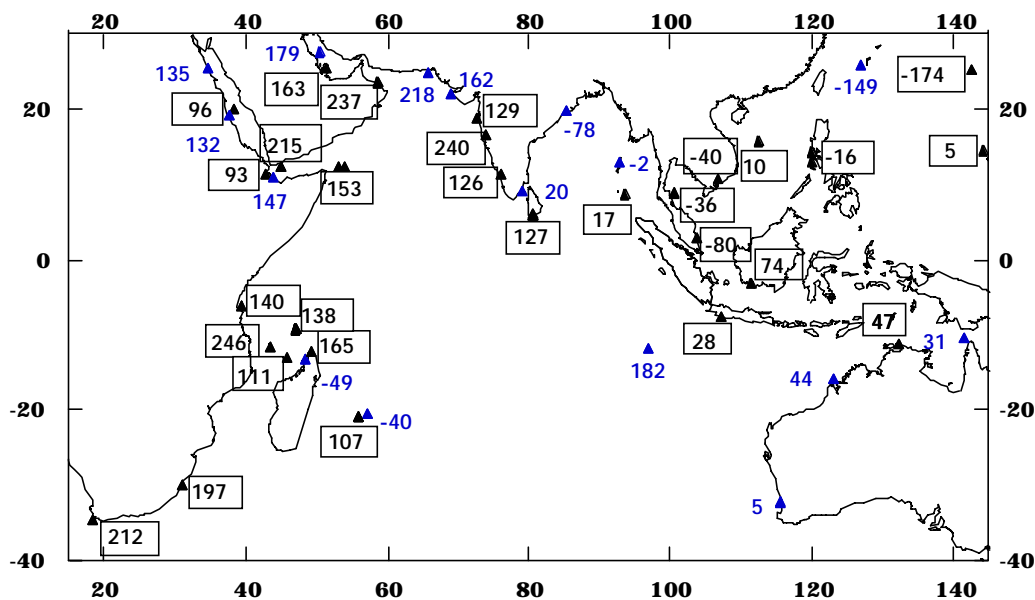
Figure 2 The geographic distribution of ΔR values. Data shown in boxes are from this study. Others are selected results from previous investigations discussed in the text, converted from their original format (conventional ages, Δ14C, etc.) to ΔR values (Stuiver and Braziunas 1993). For clarity, some data have been grouped into local averages.

The circulations of the Persian Gulf and the Red Sea are characterized by surface inflow, increases in salinity (and therefore density) through evaporation and subsequent winter cooling, and outflow of water at depth (Cember 1989). The high ΔR values in these marginal seas thus reflect those of the indrawn Arabian Sea surface water.

The northern and equatorial Indian Ocean circulation is particularly complex, with very large seasonal variations including reversals of major current systems occurring due to monsoon effects. However, in a simplified circulation scheme, the South Equatorial Current (SEC) effectively acts during the northern summer as a westward return flow south of the equator for water transported southeast from the Arabian Sea by the summer monsoon (Tchernia 1980; You 1997). The Arabian Sea gyre is then closed by northward flow along the African and Arabian coasts where the most intense upwelling occurs.

The high ΔR values from Sri Lanka are consistent with this southeast transport of 14C-depleted Arabian Sea water, assuming our samples are from the south coast (exact locations are unknown). Dutta et al. (2001) measured much higher levels of 14C in Sri Lankan samples, but those were from the shallow semi-enclosed waters of Palk Bay. This opens to the northeast on to the Bay of Bengal where they found low ΔR values (supported by our Nicobar Islands result) due to density stratification from freshwater influence. The southeast flow from the Arabian Sea extends as far east as 80–100°E south of the equator (Tchernia 1980; You 1997), and thus may also influence the high reservoir age at Cocos-Keeling at 12°S, 97°E (Toggweiler et al. 1991).

The area around Mauritius, northern Madagascar, and the Seychelles lies in the path of the SEC. Hence the summer southeast flow from the Arabian Sea may contribute to the large ΔR values in those regions also, by feeding into the eastern source regions of the SEC from the north. The winter monsoon reversal of the coastal Somali Current does not extend sufficiently far south to transport

Arabian Sea water directly into the region (Schott et al. 1990), but does feed into the eastward flow of the Equatorial Counter Current, which retroflects south into the SEC off the Indonesian coast (Michida and Yoritaka 1996; You 1997). Equatorial upwelling undoubtedly also plays a part in bringing ^{14}C-depleted water into the SEC, but this process is relatively weak in the Indian Ocean (Swallow 1984). The absence of a pronounced equatorial minimum in surface ^{14}C values in post-bomb GEOSECS and INDIGO sections and the generally reduced spatial variability of ^{14}C north of 12°S (Stuiver and Ostlund 1983; Bard et al. 1989), further suggest the importance of advection around the northern circulation relative to upwelling along its southern edge.

Water from this region north of Madagascar is transported south, via the East Mozambique Current in the east and through the Mozambique Channel in the west, into the southwest trending Aguhlas Current which retroflects eastward south of the Cape of Good Hope. The large reservoir ages along the east coast of South Africa (Natal, Cape of Good Hope) are nevertheless surprising, as more than 80% of the Aguhlas flow comes from further east (Stramma and Lutjeharms 1997), from recircula-tion south of Madagascar and from the South Indian Ocean subtropical gyre where post-bomb ^{14}C values are high (Stuiver and Ostlund 1983; Bard et al. 1989). However, hydrographic data suggest that the westernmost Aguhlas feeders have a strong influence on the inshore flow (Gordon 1986). If so, the large reservoir ages from South Africa may be due at least in part to the low ^{14}C content of the tropical source waters.

In contrast to the high ΔR values from the western Indian Ocean, our samples from the south coast of Java (Pelabuhanratu) and northern Australia's Arnhem Land (Raffles Bay) gave low ΔR values of 28 ± 70 and 47 ± 40 years, respectively. Previous results show ΔR = 44 ± 36 years for northwestern Australia (Bowman 1985) and ΔR = 35 ± 31 years for Torres Strait (Gillespie 1977; Rhodes 1980). ^{14}C values in prebomb corals from Makassar Strait, Indonesia (M K, unpublished data) and the Coral Sea (Druffel and Griffin 1993, 1999) are equivalent to ΔR close to zero. Thus, surface waters of the far western and southwestern Pacific are relatively well equilibrated with the atmosphere. Flow of these waters west through Torres Strait and south through the Indonesian Seaway (Gentilli 1972; Fieux et al. 1994; JGR 1996) gives low reservoir ages along the northwestern coast of Austra-lia and the southern coasts of the eastern Indonesian Archipelago, but evidently does not extend as far west as Cocos-Keeling (97°E). The poleward-flowing Leeuwin current (Gentilli 1972; Church et al. 1989) transports this well-equilibrated water mass along the west coast of Australia, affecting ^{14}C levels as far south as Garden Island in Western Australia at 32°S (Gillespie 1977).

Gordon (1986), Ganachaud and Wunsch (2000), and others have emphasized the importance of the warm-water route for the upper (return) limb of the global thermohaline circulation, via the Indian Ocean thermocline and the Aguhlas current (but see Schmitz [1995] for an opposing view). This return flow is associated with a ridge of minimum salinity extending westward in the thermocline from the region south of Timor to the African coast north of Madagascar (Gordon 1986; Fieux et al. 1996). The ^{14}C results from northern Australia constitute a surface signature of this movement of Pacific water west and south into the Timor Sea and beyond. However, the large ^{14}C depletions that we observe off Africa show no obvious evidence for the presence of this high-^{14}C water mass further to the west. If any Pacific "return conveyor" ^{14}C signal exists there, it either does not outcrop at the surface or is swamped by the depleted Arabian Sea component.

South China Sea

ΔR values for the South China Sea, plus some data for surrounding regions, are shown in Table 4 and Figures 2 and 3. With the exception of a single sample from Hong Kong discussed below, the South China Sea results cluster fairly well and show no obvious trends over time. The data indicate a mean

Table 4 Radiocarbon data from this study—South China Sea and Pacific

Sample codes (CAMS#)[a]	Museum#	Species (b=bivalve, c=coral, g=gastropod)	Coll. date	Location	Lat (°N)	Long (°E)	δ13C (‰)	Δ14C (‰)	±	Δ14C (Suess-corr.)[b]	14C age (BP)	±	Model age (BP)	ΔR
South/central South China Sea														
6568	USNM-309839	*Cronia margariticola* (b)	1908	Mindoro Strait, Philippines	12.5	120.5	0	−59.8	7.6	−59.8	540	70	463	77
6571	USNM-309579	*Thais distinguenda* (g)	1916[c]	Mona Is., Philippines	12.0	120.0	0	−45.6	7.7	−45.6	410	70	463	−53
8695	USNM-309529	*Gastropod*	1916	Janao Bay, Luzon, Phillipines	13.8	120.9	0	−42.9	5.6	−42.9	390	50	463	−73
49634		*Porites* (c)	1905.5	Xisha (Paracels) Is.	16.7	112.3	−2	−50.8	4.3	−50.8	460	40	463	−3
49635		*Porites* (c)	1925.5	Xisha (Paracels) Is.	16.7	112.3	−2	−50.5	5.8	−48.5	440	50	466	−26
49636		*Porites* (c)	1948.5	Xisha (Paracels) Is.	16.7	112.3	−2	−65.2	6.3	−56.2	540	60	482	58
6570	USNM-361252	*Thais hippocastaneum* (g)	1923	Ko Ang Trang, Thailand	9.6	99.7	0	−48.8	7.7	−46.8	430	70	466	−36
3956	MNHN-C31	*Gomphina aequilatera* (b)	1945	Saigon	10.8	106.8	0.3	−52.8	6.7	−44.8	440	56	480	−40
6572	USNM-17039	*Cymia gradata* (b)	1860[c]	Singapore	1.3	103.9	0	−32.8	6.0	−32.8	360	60	489	−129
3952+3961	MNHN-C27	*Marcia recens* (b)	1945	Singapore	2.9	103.8	−2.4	−53.7	4.5	−45.7	448	38	480	−32
Other														
6573	USNM-36855	*Cronia margariticola* (b)	1884[c]	Hong Kong SAR	22.2	114.2	0	−69.6	6.7	−69.6	640	60	473	167
8697	USNM-217330	*Gastropod*	1920[c]	Bo Hai Gulf, China[d]	ca. 39	ca. 119	0	−30.0	5.4	−28.0	270	50	464	−194
8814	USNM-706992	*Gastropod*	1927	Tsingtao, China	36.1	120.3	0	−41.8	6.5	−38.8	370	60	466	−96
6566	USNM-312808	*Cronia margariticola* (b)	1925[c]	SaBui Bay, S.Borneo	−3.0	111.5	0	−62.0	7.1	−60.0	540	70	466	74
8694	USNM-36238	*Gastropod*	1884	Bonin Is.	27.0	142.0	0	−29.2	6.2	−29.2	300	60	474	−174
8696	USNM-309647	*Gastropod*	1903	Guam	13.5	144.8	0	−51.6	5.5	−51.6	470	50	465	5

[a]CAMS = Center for AMS, LLNL; MNHN = Museum National d'Histoire Naturelle; USNM = National Museum of Natural History, Smithsonian Institution; H = Hong Kong Museum of History.

[b]Estimated marine fossil fuel (Suess) effect, per mil: 1959: −16 ± 4; 1952: −10 ± 2; 1949: −9 ± 3; 1945: −8 ± 2; 1925: −2 ± 2; pre-1920: ca. zero.

[c]Collected earlier, assumed date for calculation

[d]Location approximate

Table 4 Radiocarbon data from this study—South China Sea and Pacific (*Continued*)[a]

Sample codes CAMS#[a]	Museum#	Species (b=bivalve, c=coral, g=gastropod)	Coll. date	Location	Lat (°N)	Long (°E)	δ13C (‰)	Δ14C (‰)	±	14C age (BP)	±
Post-bomb data											
Hong Kong											
46198	H-64.3.52	*Bursa rana* (g)	1955	Ap Lei Chau, Hong Kong SAR	22.2	114.2	0	−32.9	4.4	260	40
46200	H-64.3.73	*Murex tribulus* (g)	1956	Ap Lei Chau, Hong Kong SAR	22.2	114.2	0	−32.4	4.4	260	40
46201	H-64.3.62	*Cypraea errones* (g)	1957	Port Shelter, Hong Kong SAR	22.4	114.3	0	−45.8	4.4	370	40
46202	H-64.3.80	*Columbella versiculor* (g)	1957	Port Shelter, Hong Kong SAR	22.4	114.3	0	−28.6	4.4	230	40
46578	H-64.3.367	*Clithon ovalaniensis* (g)	1958	Pearl Bay, Hong Kong SAR	22.5	114.3	0	−34.0	3.6	270	40
46579	H-64.3.169	*Siphonaria japonica* (g)	1959	Ap Lei Chau, Hong Kong SAR	22.2	114.2	0	−30.9	4.5	240	40
46580	H-64.3.614	*Littorina scabra* (g)	1960	High Is., Hong Kong SAR	22.4	114.3	0	16.4	4.7	>Modern	
46203	H-64.3.624	*Ostrea crenulifera* (b)	1961	NW Mirs Bay, Hong Kong SAR	22.5	114.3	0	−11.6	6.7	80	60
South/central South China Sea											
53108		*Porites* (c)	1955.4	Xisha (Paracels) Is.	16.7	112.3	−1.6	−54.9	4.0	450	40
53109		*Porites* (c)	1955.7	Xisha (Paracels) Is.	16.7	112.3	−1.8	−61.4	4.1	500	40
53110		*Porites* (c)	1956.4	Xisha (Paracels) Is.	16.7	112.3	−1.0	−58.4	3.9	480	40
53111		*Porites* (c)	1956.7	Xisha (Paracels) Is.	16.7	112.3	−3.2	−48.2	3.9	390	40
53112		*Porites* (c)	1957.4	Xisha (Paracels) Is.	16.7	112.3	−3.0	−41.3	4.2	330	40
53113		*Porites* (c)	1957.7	Xisha (Paracels) Is.	16.7	112.3	−1.0	−39.1	5.0	310	50

[a]See previous page for footnotes.

ΔR and standard error ($\sigma/\sqrt{N}$, N=10) of -25 ± 20 years for the south/central part of the Sea. ΔR values for the western Pacific and the eastern coast of China are even lower.

Like the Indian Ocean, the South China Sea circulation is strongly influenced by seasonal monsoons (Tchernia 1980). The winter monsoon drives a southwesterly flow along the northern and western coasts, fed by Pacific and East China Sea waters from the east and north, delivering water south to the Indonesian Seaway and forming the western boundary of an anti-clockwise gyre circulating between Vietnam and the Philippines. In summer the circulation is reversed, and Indonesian waters from the south feed a broad northeasterly flow that covers most of the Sea.
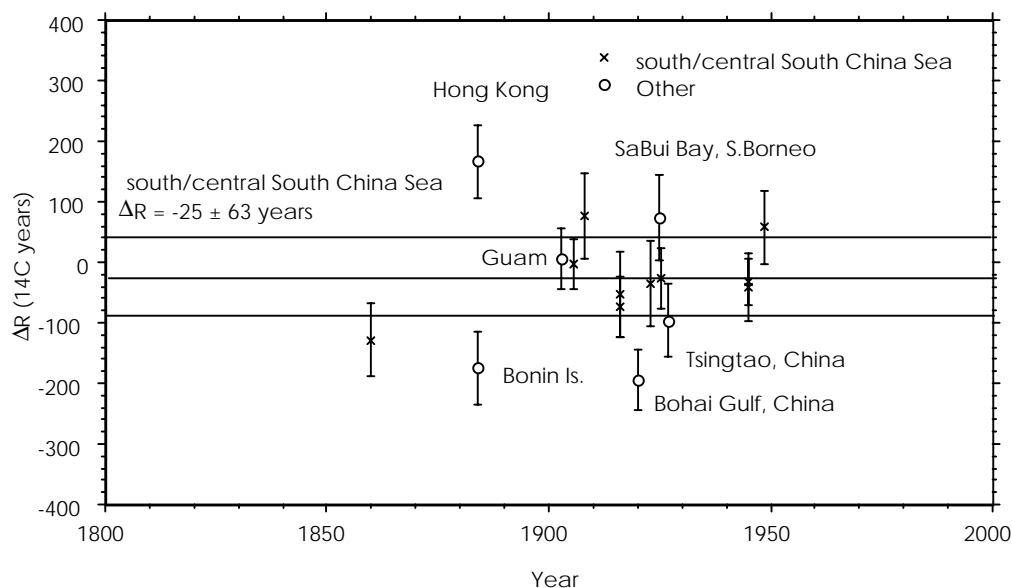
Figure 3 ΔR values for the south/central South China Sea and western Pacific, plotted against the year of collection. The Hong Kong result is high ($>2\sigma$) compared to the other South China Sea data.

The inflow from the north and east in winter is derived from the Kuroshio Current and its precursor, the Pacific North Equatorial Current (PNEC); and the low ΔR values for the islands of Okinawa and Bonin (Konishi et al. 1982; this study) attest to the high levels of ^{14}C within these waters. The origin of the summer inflow from the south is more complex. A mixture of PNEC water retroflected south in the Mindinao Current east of the Philippines (Fine et al. 1994; Gordon 1995), together with Pacific South Equatorial Current (PSEC) waters intruding into the region northwest of New Guinea in summer (Tchernia 1980), feed currents flowing south to the Indonesian Seaway, then west and north. Equatorial upwelling reduces ^{14}C levels in the PSEC compared to those found in the waters further north, but ^{14}C values for the southern edge of this current system are nevertheless relatively high (Druffel and Griffin 1993, 1999). Thus, all of the source waters entering the South China Sea are rather well equilibrated with atmospheric [14]C. Within the Sea itself, upwelling is restricted and ocean-atmosphere gas exchange enhanced, by the presence of broad shallow continental shelves and the low salinities (Levitus et al. 1994) that arise from high rainfall and surface runoff. Together, these influences produce the widespread low ΔR values.

With one exception, the South China Sea samples are from the southern and central regions. A single sample from Hong Kong (collected pre-1884) gave a high ΔR of 167 ± 60, a surprising result given

the stronger influence of Pacific and East China Sea waters in the north and the low ΔR values in those source regions. We were unable to find other pre-1950s specimens from the south China coast, but did obtain Hong Kong samples for 1955–1961. Note that even the earliest of these samples may not be truly prebomb, since there may have been early regional effects in the western Pacific from US thermonuclear tests in the Marshall Islands from 1953 onwards (Broecker et al. 1987).

Figure 4 shows Δ^{14}C data (without Suess corrections) for the Hong Kong shells, samples from the south/central South China Sea, and Okinawa corals (Konishi et al. 1982). The Okinawa and south/central South China Sea data are consistently offset over the entire period from 1915 to 1960, while the Hong Kong ^{14}C values from the late 1950s show large scatter, but generally lie within these two trend lines. On average, the Hong Kong values for 1955–56 are higher than those from farther south, corresponding to lower ΔR. On this basis, and given the uncertain collection date of the 19th century Hong Kong sample, we discount that result and suggest that ΔR for the South China coast probably lies between the values of –25 ± 20 for the waters to the south and –149 ± 7 for Okinawa (Konishi et al. 1982). However, the true value will only be determined when pre-1950 samples become available.
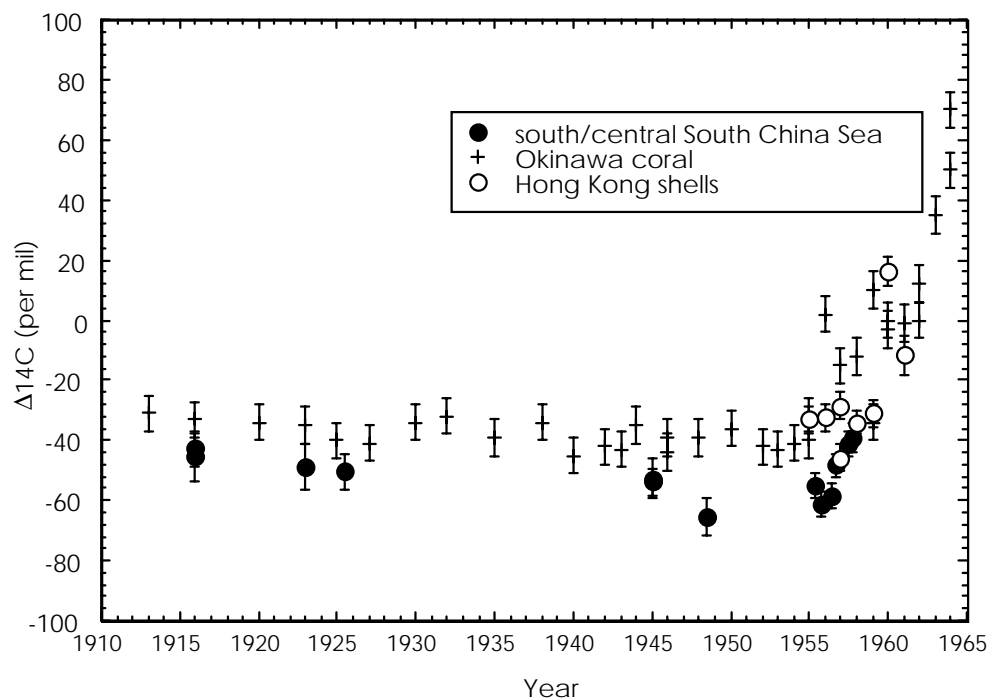

Figure 4 Δ^{14}C values for the period 1910–1965, plotted without Suess correction. Okinawa values are consistently higher than those from the south/central South China Sea. Hong Kong data from the late 1950s generally fall between these two trends.

CONCLUSIONS

Surface waters over large areas of the western Indian Ocean are significantly influenced by Arabian Sea upwelling, with regional ΔR mean values ranging from 140 to 205 years. These results contrast with data from southern Java and northern Australia which show ΔR values of 50 years or less. This difference is explained by the presence of well-equilibrated water masses in the western Pacific, which flow into the eastern Indian Ocean via Torres Strait and the Indonesian Seaway. The South

China Sea is also strongly influenced by these high-^{14}C Pacific waters, and ΔR values for the south/central part of the Sea are close to zero. Post-bomb results for Hong Kong suggest that ΔR values along the South China coast may be even lower.

ACKNOWLEDGMENTS

REFERENCES

Bard E, Arnold M, Toggweiler JR, Maurice P, Duplessy J-C. 1989. Bomb ^{14}C in the Indian Ocean measured by accelerator mass spectrometry: oceanographic implications. *Radiocarbon* 31(3):510–22.

Bhushan R, Chakraborty S, Krishnaswami S. 1994. Physical Research Laboratory (Chemistry) radiocarbon date list I. *Radiocarbon* 36(2):251–6.

Bowman GM. 1985. Oceanic reservoir correction for marine radiocarbon dates from northwestern Australia. *Australian Archaeology* 20:58–67.

Broecker WS. 1963. ^{14}C/^{12}C ratios in surface ocean water. U.S. National Academy of Sciences, National Research Council publication 1075:138–49.

Broecker WS, Cember RP, Toggweiler JR, Trumbore SE, White J. 1987. Final Report on the Lamont-Doherty geological Observatory coral radioisotope project. DOE/EV/10041C-1 (unpublished).

Cember R. 1989. Bomb radiocarbon in the Red Sea: a medium-scale gas exchange experiment. *Journal of Geophysical Research* 94:2111–23.

Church JA, Cresswell G, Godfrey JS. 1989. The Leeuwin Current. In: Neshyba SJ, Mooers ChNK, Smith RL, Barber RT, editors. *Poleward flow along eastern ocean boundaries.* Coastal and Estuarine Studies 34. New York: Springer-Verlag. p 230–54.

Delibrias G. 1980. Carbon-14 in the Southern Ocean. *Radiocarbon* 22(3):684–92.

Druffel, ERM. 1997. Pulses of rapid variation in the North Atlantic surface ocean during the past century. *Science* 275:1454–7.

Druffel ERM, Griffin S. 1993. Large variations of surface ocean radiocarbon: evidence of circulation changes in the southwestern Pacific. *Journal of Geophysical Research* 98: 20249–59.

Druffel ERM, Griffin S. 1999. Variability of surface ocean radiocarbon and stable isotopes in the southwestern Pacific. *Journal of Geophysical Research* 104: 23607–13.

Druffel ERM, Suess H. 1983. On the radiocarbon record in banded corals. *Journal of Geophysical Research* 88: 1271–80.

Dutta K, Bhushan K, Somayajulu BLK. 2001. ΔR correction values for the northern Indian Ocean. *Radiocarbon* 43(2):483–8.

Dye T. 1995. Apparent ages of marine shells: implications for archaeological dating in Hawai'i. *Radiocarbon* 36(1):51–7.

Fieux M, Andrie C, Delecluse P, Ilahude AG, Kartavtseff A, Mantisi F, Molcard R, Swallow JC. 1994. Measurements within the Pacific-Indian oceans flowthrough region. *Deep Sea Research* 41: 1091–130.

Fieux M, Andrie C, Charriaud E, Ilahude AG, Metzel N, Molcard R, Swallow JC. 1996. Hydrological and chlorofluoromethane measurements of the Indonesian flowthrough entering the Indian Ocean. *Journal of Geophysical Research* 101:12433–54.

Fine RA, Lukas R, Bingham FM, Warner MJ, Gammon RH. 1994. The western equatorial Pacific: a water mass crossroads. *Journal of Geophysical Research* 99: 25063–80.

Ganachaud A, Wunsch C. 2000. Improved estimates of global ocean circulation, heat transport and mixing from hydrographic data. *Nature* 408:453–7.

Gentilli J. 1972. Thermal anomalies in the Eastern indian Ocean. *Nature Physical Science* 238:93–5.

Gillespie R. 1977. Sydney University natural radiocarbon measurements IV. *Radiocarbon* 19(1):101–10.

Gordon AL. 1986. Interocean exchange of themocline water. *Journal of Geophysical Research* 91: 5037–46.

Gordon AL. 1995. When is "appearance" reality? Indonesian flowthrough is primarily derived from N. Pacific water masses. *Journal of Physical Oceanography* 25:1560–7.

Ingram L, Southon JR. 1996. Reservoir ages in eastern Pacific coastal and estuarine water. *Radiocarbon* 38(3):573–82.

JGR. 1996. Special session: Pacific low-latitude western boundary currents and the Indonesian flowthrough. *Journal of Geophysical Research* 101:12209–488.

Konishi K, T.Tanaka T, Sakanoue M. 1982. Secular variation of radiocarbon concentrations in seawater: Sclerochronological approach. In: Gomez ED, editor. *Pro-*

ceedings of the Fourth International Coral Reef Symposium. Volume 1. Manila: Marine Science Center, University of the Phillipines. p 181–5.

Levitus S, Burgett R, Boyer TP. 1994. *World ocean atlas volume 3: salinity.* NOAA Altas NESDIS 3. Washington DC: US Department of Commerce.

Loyd DH, Vogel JS, Trumbore S. 1991. Lithium contamination in AMS measurements of [14]C. *Radiocarbon* 33(3):297–301.

Michida Y, Yoritaki H. 1996. Surface currents in the area of the Indo-Pacific flowthrough and in the tropical Indian Ocean. *Journal of Geophysical Research* 101: 12475–82.

Rhodes EG, Polach HA, Thom BG, Wilson SR. 1980. Age structure of Holocene coastal sediments: Gulf of Carpentaria, Australia. *Radiocarbon* 22(3):718–27.

Schmitz WJ. 1995. On the interbasin-scale thermohaline circulation. *Reviews of Geophysics* 33:151–73.

Schott F, Swallow JC, Fieux M. 1990. The Somali Current at the equator: annual cycle of currents and transports in the upper 1000m and connection to neighbouring latitudes. *Deep Sea Research* 37: 11825–48.

Southon JR, Caffee MW, Davis JC, Moore TL, Proctor ID, Schumacher B, Vogel JS. 1990. The new LLNL AMS spectrometer. *Nuclear Instruments and Methods in Physics Research* B52:301–5.

Stramma L, Lutjeharms JRE. 1997. The flow field of the subtropical gyre of the South Indian Ocean. *Journal of Geophysical Research* 102:5513–30.

Stuiver M, Polach, H. 1977. Reporting of ^{14}C data. *Radiocarbon* 19(3):355–63.

Stuiver M, Braziunas TF. 1993. Modeling atmospheric ^{14}C influences and ^{14}C ages of marine samples to 10,000 BC. *Radiocarbon* 35(1):137–89.

Stuiver M, Ostlund, HG. 1983. GEOSECS Indian Ocean

and Mediterranean radiocarbon. *Radiocarbon* 25(1): 1–29.

Stuiver M, Pearson GW, Braziunas TF. 1986. Radiocarbon age calibration of marine samples back to 9000 cal BP. *Radiocarbon* 28(2B):980–1021.

Stuiver M, Reimer PJ, Braziunas TF. 1998. High-precision radiocarbon age calibration for terrestrial and marine samples. *Radiocarbon* 40(3):1127–51. (Data available on the Internet at http://www.calib.org/marine).

Swallow JC. 1984. Some aspects of the physical oceanography of the Indian Ocean. *Deep Sea Research* 31: 639–50.

Tchernia P. 1980. *Descriptive regional oceanography.* Pergamon, Oxford University Press.

Toggweiler R, Dixon K, Broecker WS. 1991. The Peru upwelling and the ventilation of the South Pacific thermocline. *Journal of Geophysical Research* 96:20467–97.

Toole JM, Warren BA 1993. A hydrographic section across the subtropical South Indian Ocean, *Deep Sea Research* 40:1973–2019.

Vogel JS, Nelson DE, Southon JR. 1987. [14]C background levels in an AMS system. *Radiocarbon* 29(3):323–33.

von Rad U, Schaff M, Michels KH, Berger WH, Siricko F. 1999. A 5000-yr record of climate change in varved sediments from the oxygen minimum zone off Pakistan, northeastern Arabian Sea. *Quaternary Research* 51:39–53.

Wrytki K. 1973. Physical oceanography of the Indian Ocean. In: Zeitschel B, editor. *The biology of the Indian Ocean.* New York: Springer-Verlag. p 18–36.

You Y. 1997. Seasonal variations of themocline circulation and ventilation in the Indian Ocean. *Journal of Geophysical Research* 102: 10391–422.